

EFFECT OF JET LENGTH ON PRESSURE FLUCTUATIONS IN $\frac{3}{4}$ OPEN-JET WIND TUNNELS

Dr. Mark Rennie
Aero-Acoustics Engineering Group
Aiolos Engineering Corporation
Toronto, Canada

SYNOPSIS

A well-known problem associated with open-jet wind tunnels is that of test chamber static pressure fluctuations, that can reduce the simulation quality or even limit the effective wind speed range of a facility. These pressure fluctuations are normally attributed to a coupling between large-scale coherent vortices shed from the nozzle and wind tunnel resonant modes; however, the exact mechanism of the interaction is not fully understood. In an effort to identify the important design parameters for open-jet test sections, an experimental investigation into the cause of pressure fluctuations in open-jet wind tunnels was undertaken. For the investigation, a $1/7^{\text{th}}$ -scale model of a $\frac{3}{4}$ open-jet automotive wind tunnel test section was constructed and integrated into an existing closed-circuit wind tunnel. Data in the form of root-mean-square fluctuating C_p amplitudes ($C_{p\text{rms}}$) and pulsation frequency, plotted as a function of wind speed, are presented, and indicate a strong correlation between the frequency of pressure disturbances and the length of the free jet. The implications of this result on a mechanism for the pressure fluctuations are discussed.

NOMENCLATURE

A_c - collector area
 A_n - nozzle area
 c - speed of sound
 $C_{p\text{rms}}$ - root-mean-square pressure coefficient associated with pressure fluctuations
 D_h - nozzle hydraulic diameter
 f - frequency
 l_x, l_y, l_z - plenum dimensions
 L_{circ} - wind tunnel circuit length
 L_{jet} - jet length (distance from nozzle lip to collector inlet)
 L_{noz} - nozzle length
 St - Nondimensional frequency, Strouhal number
 t_d - time for pressure disturbance to travel from collector to nozzle
 t_v - time for vortex to convect from nozzle to collector inlet
 U - test-section wind speed

V - plenum volume

1 INTRODUCTION

The problem of jet pulsations in open-jet wind tunnels has received increased attention in the recent literature (1 - 4). This attention may be driven by an increased awareness of the effects that pressure fluctuations have on data quality and wind tunnel operation (3, 5).

For the wind tunnel designer, the problem of eliminating or minimizing pressure fluctuation levels is therefore a serious one. At present, the general design criterion for a new, state-of-the-art, open-jet wind tunnel is that the root-mean-square pressure coefficient (C_{prms}) associated with pressure fluctuations should be less than 0.005 over the entire operating wind speed range. The design for low pressure fluctuation levels can be aggravated, however, by the desire for longer test sections in order to improve simulation quality or to accommodate a range of facility test missions. Finally, jet pulsations, although typically occurring at much lower than acoustic frequencies, can still detrimentally impact background noise levels during aero-acoustic testing, due to higher-frequency noise associated with an unsteady jet mass flow.

In an effort to more fully understand the mechanisms behind wind tunnel pulsations, Aiolos Engineering Corporation has recently undertaken an experimental investigation into the causes of low-frequency pressure pulsations in open-jet automotive wind tunnels. The investigation was performed using a 1/7th-scale model of a closed-circuit wind tunnel, with an open-jet test section that was representative of current designs. The first stage of the test program concentrated on the effect of test-section length. The objective of the test program was to generate an increased understanding of the effect of test-section length on jet pulsation levels and frequencies, that might lead to design guidelines for future wind tunnels.

2 EXPERIMENT

The experimental program was performed in the Pilot Wind Tunnel (PWT) at the Institute for Aerospace Research laboratory of the National Research Council, Canada. The wind tunnel was modified from its original configuration for the testing, with the test leg replaced by a 1/7th-scale model of the settling chamber, a 6:1 contraction, test section and test-section diffuser of a typical open-jet automotive wind-tunnel for aero-acoustic testing. Although the remainder of the PWT circuit was unchanged, it very closely matched the scale and dimensions of the return circuit of an aero-acoustic wind tunnel. With the model insert, the maximum wind speed of the facility was 200 kph, which is also representative of present facilities. A drawing of the wind tunnel circuit is shown in Figure 1.

The model test section had a rectangular nozzle with dimensions 0.571 m x 1.0 m; corresponding to a full-scale nozzle area of 28 m². The collector throat was also rectangular in shape and was fitted with hinged collector flaps to give control over the collector inlet area. The collector flaps were rectangular in shape, and had bell-mouthed leading edges consisting of half cylinders with 0.07 m radius. In its basic configuration, the jet length (distance from nozzle lip to collector inlet) was 2.54 m, for a nondimensional jet length (L/D_h) of 3.5.

The jet length could be varied by inserting straight-duct spacers between the test-section diffuser inlet and the collector flaps. Two different spacer lengths were tested, giving jet lengths of 1.92 m and 2.28 m ($L/D_h = 2.64, 3.14$). The test-section plenum dimensions of 3.8 m x 2.4 m x 1.3 m

were optimized for the largest, baseline jet length of 2.54 m, and were not varied for the different jet lengths tested. Not adjusting the plenum size for the different jet lengths was expected to introduce negligible error to the results.

Pressure fluctuations were measured using a single Setra model 238 differential pressure transducer with 0.1 psi range. The transducer was mounted in the plenum out of the jet, approximately halfway between the nozzle and collector, with its front face exposed to the plenum air. All measurements were made at this single location, and, since fluctuation amplitudes may be expected to vary spatially within the test-section (4), the final results may not represent an accurate evaluation of the average fluctuation amplitude. The relative fluctuation amplitudes can still be used, however, to compare the effect of different test-section configurations.

A long length of plastic pressure tubing was attached to the reference port of the transducer and terminated in the external (outside of plenum) ambient air. This pressure tubing acted as a simple low-pass, essentially DC filter. Pressure spectra were measured using an HP-35655A spectrum analyzer.

2.1 Frequency Range

Test parameters, such as the frequency range of the measurements, were determined from an analysis of the problem physics. The analysis presented below is not new but can be found, for example, in References (1) and (3); however, it is tailored to the specific details of our test setup.

Large-amplitude, test-section pressure fluctuations occur when the frequency of unsteady forces associated with the jet correspond to wind tunnel resonant modes. Jet unsteady forces originate with large vortex structures that are shed from the nozzle lip, which have been found to naturally populate the shear layer of a free jet (6). For a fully-open jet with rectangular nozzle, the preferred frequency for this “natural” vortex shedding is $St \approx 0.48$ (3, 7). This result can be extended to the case of a $3/4$ -open jet by treating the test-section floor as a reflection plane. The nozzle hydraulic diameter is therefore effectively increased by a factor of approximately $\sqrt{2}$; however, in practice, it is simpler to maintain the conventional definition for the nozzle hydraulic diameter, and instead reduce the effective Strouhal number for natural shedding by a factor of $\sqrt{2}$, giving $St \approx 0.34$ (3).

Wind tunnel resonant frequencies are well described in (1) and (3):

1. Circuit resonant frequencies, neglecting end corrections, are:

$$f = \frac{nc}{2L_{\text{circ}}} \quad (1)$$

For our wind tunnel, with circuit length of 28.6 m, the first mode occurs at 6 Hz.

2. Plenum resonances are calculated using

$$f = \frac{c}{2\sqrt{\left(\frac{l_x}{n_x}\right)^2 + \left(\frac{l_y}{n_y}\right)^2 + \left(\frac{l_z}{n_z}\right)^2}} \quad (2)$$

Based on the longest plenum dimension of 3.8 m (see above), plenum resonances begin at a frequency of 45 Hz.

3. The nozzle and test-section plenum can also create a Helmholtz-type resonance. According to (3), choosing realistic values from which to estimate Helmholtz frequencies for an open-jet configuration involves considerable guesswork; however, the following was suggested:

$$f = \frac{c D_h}{4\pi} \sqrt{\frac{\pi}{V \left(L_{noz} + \pi \frac{D_h}{4} \right)}} \quad (3)$$

Using a nozzle length L_{noz} of 0.4 m, Equation (3) gives a frequency of 10.3 Hz.

4. Finally, an edgetone-type feedback can occur, as described recently in (8). In this case vortex interaction with the collector generates a pressure disturbance that travels back to the nozzle to stimulate the shedding of follow-on vortices. The existence of the edgetone feedback mechanism in low-speed wind tunnels was recognized as early as 1958 (9), and a good review of edgetone feedback mechanisms is given in (10), which lists several incompressible-flow examples.

With a top wind speed of 200 kph, the maximum frequency of natural vortex shedding is 26 Hz. An examination of the possible circuit resonances given above shows that, with the exception of the fairly speculative prediction of Equation (3), the full circuit resonance is the only type of resonance that is likely to be excited; other resonance modes occur at too high a frequency. Since model-scale vortex-shedding and resonant frequencies are both simply related to full-scale values by the scale factor, this conclusion holds equally well for a full-scale analysis. Although it is by no means implied that other resonant modes can be ignored, the above analysis clearly indicates the importance of including the wind tunnel return leg in any experimental investigation of open-jet pressure fluctuations.

Based on the above analysis, pressure fluctuation spectra were measured over the range 0 – 25 Hz. Some spectra were also acquired in the range 0 - 50 Hz.

2.2 Results

Start-up tests made in the completed model-scale wind tunnel showed immediately that jet pulsations existed over the entire wind speed range up to 200 kph. An example of a spectrum measured with the baseline 2.54 m jet length, acquired at a test-section wind speed of 130 kph, is shown in Figure 2. More than one peak can be observed in the spectrum, indicating that more than one resonant mode was simultaneously excited. This was found to be a fairly common occurrence in the data; however, the spectra were typically dominated by just one of the peaks.

The dependence of C_{prms} pressure fluctuation amplitudes on wind speed are plotted in Figure 3, for the tested jet lengths of 2.54 m, 2.28m and 1.92 m ($L/D_h = 3.5, 3.14, 2.64$). Only the magnitude of the largest-amplitude C_{prms} peak at any wind speed is plotted. An evaluation of the uncertainty associated with the data was performed by repeating 3 test runs using the baseline 2.54 m jet configuration. Due to the small data base, a statistical evaluation of the error was not attempted; however, C_{prms} levels generally repeated within ± 0.005 . A range of ± 0.005 is denoted by the error bars shown in Figure 3.

2.2.1 Collector Area

Since constant-area spacers were used to control the jet length, the collector throat area remained the same for all three jet lengths. The collector inlet area could be varied, however, by changing the collector flap angles. To investigate the effect of collector inlet area on pressure fluctuations, some tests were repeated with the collector area set to different values. The investigation was not extensive, but was undertaken merely to obtain an idea of the sensitivity of the amplitude of pressure fluctuations to the collector area.

Figure 3 includes Cprms amplitudes for two different collector areas for the 2.28 m and 1.92 m jet lengths. For the 2.28 m jet, Cprms levels up to 0.03 were found to exist when the collector was set to $A_c/A_n = 1.56$; however, when the collector area was increased by 15%, Cprms levels decreased below 0.01 over the full wind speed range. For the 1.92 m jet, a collector area of $A_c/A_n = 1.54$ was found to produce Cprms levels below 0.005 over most of the wind speed range, but increased when the collector area was reduced by 14%. Collector area effects were not investigated for the 2.54 m jet; this is because the collector area could not be substantially increased beyond the optimum area, and smaller collector areas were not investigated due to the already large amplitude of the pressure fluctuations and attendant concern for causing damage to the model. However, from Figure 3 it is evident that the amplitude of Cprms fluctuations increases when the collector inlet area is decreased.

In general, Figure 3 shows that the level of pressure pulsations becomes more severe as the jet length is increased. This result is not new, but has been reported, for example, in Reference 4, and can be attributed to the thickening of the jet shear layer with increasing jet length and its attendant increase in turbulent energy. In the next section, further insight into the data is gained by examining the frequencies associated with the pressure fluctuations.

2.2.2 Frequencies

The frequencies of the measured pressure fluctuations are plotted in Figure 4. The figure shows the frequencies of all spectral peaks measured at each wind speed. Figure 4 shows that the pressure fluctuation frequencies tend to occur in four horizontal bands at the following four frequencies: 4 Hz, 12 Hz, 18 Hz, and 24 Hz. These frequencies correspond very well to the first four circuit modes, Equation (1), indicating that the pressure fluctuations were probably all associated with excitation of the wind tunnel full-circuit resonant modes.

In Figure 4, the frequencies of the largest-amplitude pressure fluctuations are circled with dashed lines, and these correspond to the maximum Cprms levels shown in Figure 3. Hence, for example, the large-amplitude Cprms peaks at 90 kph and 180 kph in Figure 3 occur at frequencies of roughly 12 Hz and 24 Hz respectively. Figure 4 shows that the Cprms peak that occurs at 40 kph has a frequency of either 4 Hz or 12 Hz, while the peak at around 140 kph occurs at either 12 Hz or 18 Hz. No explanation is given for this apparent sharing of energy between tunnel modes.

Figure 4 also shows the curve for natural vortex shedding, $St = 0.34$. The large-amplitude pressure fluctuation peaks (dashed ovals) generally occur at the intersections of the $St = 0.34$ line with the wind tunnel circuit modes.

Based on the above evidence, it might be concluded that the pressure fluctuations are caused by a simple coupling between natural vortex shedding from the nozzle lip, and the wind tunnel circuit modes. Closer examination of Figure 4 shows, however, a finer structure to the data, which is that the frequencies of the pressure fluctuations are, in fact, differentiated according to jet length.

This is particularly noticeable in the data for wind speeds greater than 100 kph where, at any given wind speed, the fluctuations for the 2.54 m jet occur at lower frequencies than for the 2.28 m and 1.92 m jets, the fluctuations for the 2.28 m jet occur at middle frequencies, and the fluctuations for the 1.92 m jet occur at the highest frequencies. This splitting of fluctuation frequencies is denoted in Figure 4 for a wind speed of 120 kph.

The clue to the origin of this frequency separation is that the separation is not arbitrary, but rather, scales with the jet length. Hence, at any particular wind speed,

$$\frac{f L_{\text{jet}}}{U} \approx \text{constant} \quad (4)$$

that is, it is possible to form a Strouhal number from the jet length. This indicates that the time for a disturbance to convect from the nozzle to the collector is an important parameter, which suggests the existence of edgetone-type feedback as briefly described in Section 2.1. The influence of the collector on pressure fluctuation amplitudes has already been described, and lends further support to the hypothesis of edgetone feedback. In order to check this hypothesis, a simple model for edgetone feedback resonance was constructed and compared to the data; the development of this model is described in the following section.

3 EDGETONE FEEDBACK MODEL

The edgetone feedback loop has been described in (8 - 10). The loop begins with a coherent vortex shed from the nozzle lip which convects downstream until it contacts the collector. This interaction generates a pressure disturbance which propagates back upstream, and the loop is closed when the disturbance reaches the nozzle, causing a new vortex to be shed. The frequency of the feedback mechanism can be predicted from a simple analysis of the time required for each phase of the feedback loop.

Starting with the vortex shedding from the nozzle lip, the convection speed of a vortex in the shear layer of an open jet is approximately 65% of the wind speed in the core. The time required for the vortex to reach the collector is thus

$$t_v = \frac{L_{\text{jet}} + \Delta l}{0.65 U} \quad (5)$$

The length Δl in Equation (5) accounts for the fact that there is uncertainty regarding the exact streamwise location in the collector at which the vortex interacts with the collector walls and generates a pressure disturbance. It will be shown below that the value of Δl required to match the experimental data is only a small perturbation on the actual jet length L_{jet} .

Once created, it is possible for the pressure disturbance to travel to the nozzle either back through the flow, or through the essentially still air in the plenum surrounding the flow. According to (8), the preferred path for the upstream-propagating disturbance is through the flow. As shown below, this path gives results that more closely match the experimental data.

Propagating upstream through the flow, the speed of the returning pressure disturbance is retarded by the flow speed. The time for the disturbance to reach the nozzle is therefore

$$t_d = \frac{L_{jet} + \Delta l}{c - U} \quad (6)$$

The total time to complete the feedback loop is the sum of t_v and t_d , and the frequency is obtained by taking the reciprocal:

$$f = \frac{1}{t_v + t_d} = \frac{1}{\frac{L_{jet} + \Delta l}{0.65 U} + \frac{L_{jet} + \Delta l}{c - U}} \quad (7)$$

Note that, at the wind speeds tested, $t_v \gg t_d$, and it therefore might be argued that Equation (7) could be simplified by neglecting t_d without loss of accuracy; however t_d was included because, as shown below, it gives a perturbation to the predicted resonant frequencies that more closely matches the experimental data.

Initial calculations performed using Equation (7) gave, however, frequencies much lower than the measured frequencies. The reason for this discrepancy is the relatively slow convection speed of the downstream-traveling vortices. This is easily shown by momentarily neglecting the (small) correction Δl , and the time t_d , in which case Equation (7) reduces to

$$f = \frac{0.65 U}{L_{jet}} \quad (8)$$

Nondimensionalizing by windspeed and nozzle diameter gives a Strouhal number of

$$St = \frac{0.65}{\left(\frac{L_{jet}}{D_h}\right)} \quad (9)$$

For the nondimensional jet lengths that we tested, this is in the range $St \approx 0.19$ to 0.25 , which represents much lower frequencies than the natural vortex shedding at $St = 0.34$; as shown in Figure 4, the largest-amplitude pressure fluctuations occur fairly close to the $St = 0.34$ line.

There is, however, no physical reason that two or more vortices cannot exist in the test section simultaneously. In fact, for typical open-jet test-section lengths, it is a simple exercise to show that this is actually a normal situation. To understand this idea, it must first be realized that there is no natural mechanism to initiate the nozzle-collector feedback loop. Instead, the feedback loop probably starts with natural vortex shedding from the nozzle at the normal Strouhal frequency of 0.34 . In this case, the separation between vortices (or vortex “wavelength”) is obtained by dividing the convection speed by the natural vortex shedding frequency:

$$\lambda = \frac{0.65 U}{f} = \frac{0.65 U}{\left(\frac{St U}{D_h}\right)} = 1.91 D_h \quad (10)$$

The number of vortices resident in the test section at any one time is then obtained by dividing the jet length by the vortex separation λ :

$$n = 0.52 \left(\frac{L_{\text{jet}}}{D_h} \right) \quad (11)$$

Therefore, for nondimensional jet lengths of approximately 2 or greater, (the case for many open-jet wind tunnels), Equation (11) demonstrates that the jet is so long that the nozzle “naturally” generates a second vortex before the first vortex reaches the collector.

With two vortices resident in the test section, the pressure disturbance generated by any vortex stimulates the generation of the second following vortex, rather than the immediately following vortex. Otherwise, initiation of the nozzle-collector feedback loop proceeds normally. The second vortex is most likely generated out of phase with the natural vortex shedding, however, with the feedback loop established, the nozzle shedding no longer follows the natural shedding frequency, but rather “locks” in to the frequency dictated by the feedback loop. A diagram of the final feedback mechanism is shown in Figure 5.

With n vortices resident in the test section, the distance that any vortex travels in one shedding period is now roughly equal to the jet length divided by n . Equation (5) thus becomes:

$$t_v = \left(\frac{1}{n} \right) \frac{L_{\text{jet}} + \Delta l}{0.65 U} \quad (12)$$

The feedback frequency is therefore:

$$f = \frac{1}{\left(\frac{1}{n} \right) \frac{L_{\text{jet}} + \Delta l}{0.65 U} + \frac{L_{\text{jet}} + \Delta l}{c - U}} \quad (13)$$

In Section 3.1 below, n was set to 2 for the specific case of two vortices resident in the test section.

3.1 Comparison of Model with Experimental Data

Before comparing Equation (13) to the experimental data, it was first necessary to determine a value for the “collector interaction length,” Δl . Although there is no physical reason that Δl cannot have a different value depending on jet length (and collector flap setting angle), it was decided to seek a single value for Δl that minimized the difference between Equation (13) and the experimental data for all three jet lengths. The value for Δl determined in this manner was 0.1 m. Although any statement here on the physics of the interaction of a vortex with the collector walls must be regarded as speculative, the result $\Delta l = 0.1$ m implies that the vortex travels only a short distance into the collector before interacting with the collector walls and creating a pressure disturbance. In any case, based on the overall collector length of 0.8 m, the value of 0.1 m for the collector interaction length appears reasonable.

Using $\Delta l = 0.1$ m, the edgetone feedback frequency curves predicted by Equation (13) are plotted in Figure 6. The figure shows reasonably good agreement between Equation (13) and the experimental data. Of particular interest is the downward-curving trend of the curves generated by Equation (13), which accurately reproduces the trend of the data. This downward-curving trend can be traced to the t_d term, Equation (6), demonstrating the importance of modeling the disturbance propagation time even at the low wind speeds tested here.

4 SUMMARY AND CONCLUSIONS

This paper has presented evidence pointing to the existence of edgetone-type feedback in open-jet wind tunnels at low wind speeds:

- Jet pulsation frequencies were found to scale with jet length at any particular wind speed.
- The amplitude of pressure pulsations was found to be sensitive to collector inlet area.

This evidence culminated in the development of a simple model for predicting edgetone feedback frequencies, which reproduced the experimental data with reasonable accuracy.

The investigation used simple, rectangular collector flaps with bell-mouthed leading edges; however, the results should still be relevant for other collector shapes as described, for example, in (11). If so, then the results may give additional insight into the success of common methods used to control jet pulsations. For example, although not described in this paper, it was found that pressure pulsation amplitudes for the 2.54 m jet could be reduced below 0.01 at all wind speeds, and below 0.005 over most of the wind speed range, by introducing a small breather gap at the downstream edge of the collector. It is possible that this breather gap may function by reducing the strength of the pressure disturbances created when downstream-convecting vortices impact the collector walls, thus disrupting the edgetone feedback.

Large-amplitude pressure fluctuations in open-jet wind tunnels can be traced to a wide variety of sources. This research has re-emphasized the importance of considering jet length in any investigation of pressure fluctuations, and that the complete physics of the phenomenon may not be captured using prediction methods based on nozzle dimensions alone.

References

1. Holthusen, H., Kooi, J. W., "Model and Full Scale Investigations of the Low Frequency Vibration Phenomenon of the DNW Open Jet," AGARD-CP-585, 1997
2. Ginevsky, A. S., "Self-Oscillation Flow Control in Free-Jet Wind Tunnels," AGARD-CP-585, 1997
3. Wickern, G., von Heesen, W., and Wallmann, S., "Wind Tunnel Pulsations and their Active Suppression", SAE 2000-01-0869, 2000.
4. Arnette, S. A., Buchanan, T. D., and Zabat, M., "On Low-Frequency Pressure Pulsations and Static Pressure Distribution in Open jet Automotive Wind Tunnels," SAE 1999-01-0813, 1999.
5. Van Ditshuizen, J. C. A., Holthusen, H., "Review and prospects for Aeroacoustic Testing at NW," DNW Report.
6. Crow, S. C., and Champagne, F. H. "Orderly Structure in jet Turbulence," Journal of Fluid Mechanics, vol. 48, part 3, pp.547 – 591, 1971.
7. Michel, U., Froebel, E. "Turbulence at Far Downstream Positions in the Open Working Section of the German-Dutch Wind Tunnel DNW," DLR IB-2214-85/B10, 1985.

8. Ahuja, K. K., Massey, K. C., and D'Agostino, M. S., Flow/Acoustic Interactions in Open-Jet Wind Tunnels, AIAA Paper 97-1691, 1997.
9. King, J.L, Boyle, P., Ogle, J. B., "Instability in Slotted Wall Tunnels," *Journal of Fluid Mechanics*, Vol. 4, 1958, pp 283 – 305.
10. Rockwell, D., "Oscillations of Impinging Shear Layers," *AIAA Journal*, Vol.21, No.5, 1983.
11. Manuel, G. S., Molloy, J. K., and Barna, P. S., "Effect of Collector Configuration on Test Section Turbulence Levels in an Open-Jet Wind Tunnel," NASA TM-4333, 1992.

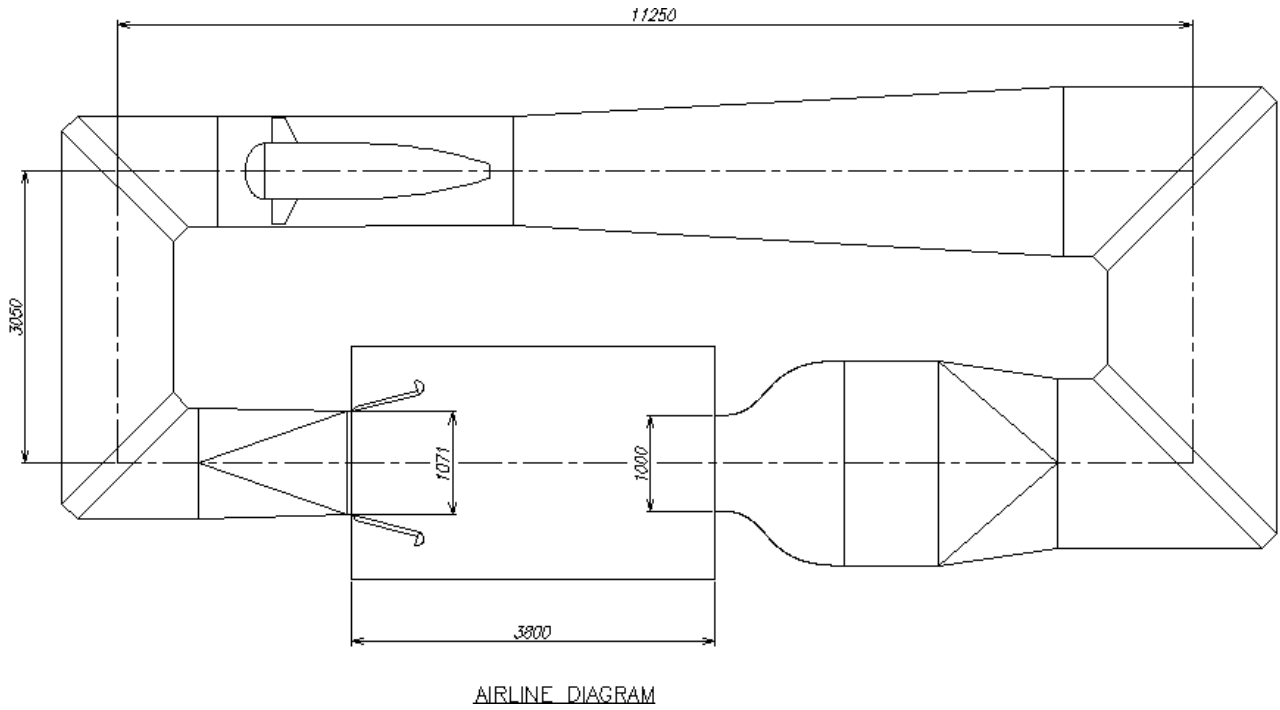


Figure 1: Diagram of wind tunnel circuit.

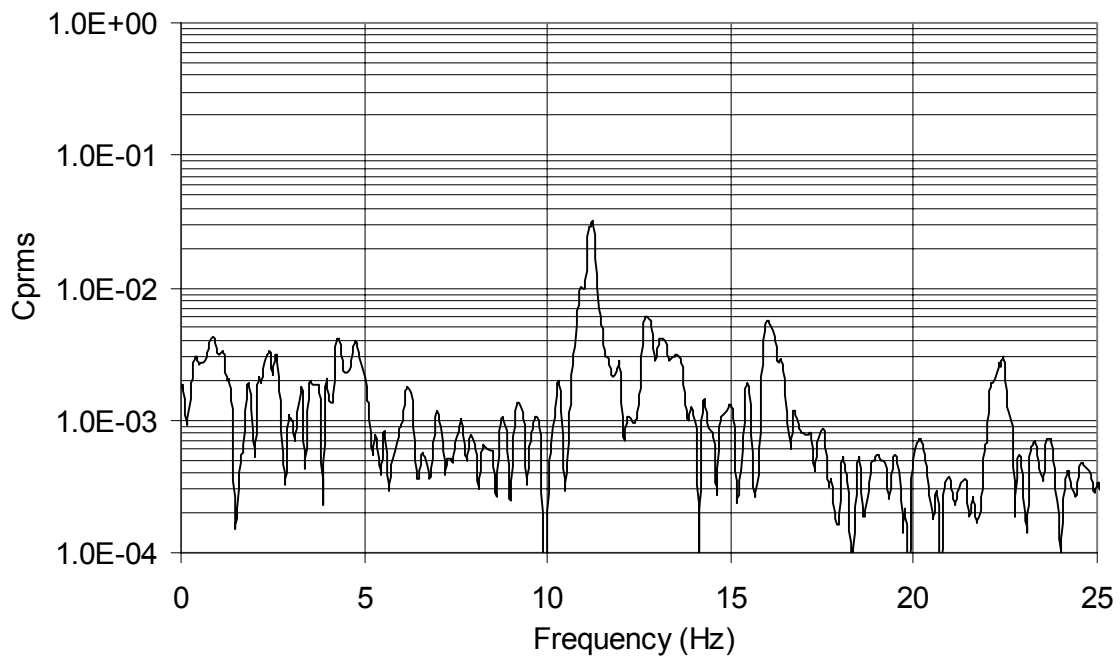


Figure 2: Typical spectra of pressure pulsations; 2.54 m jet, 130 kph.

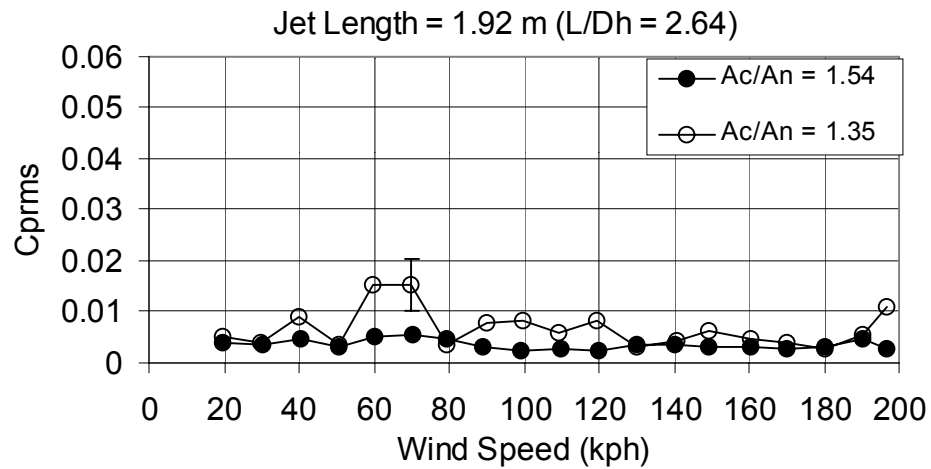
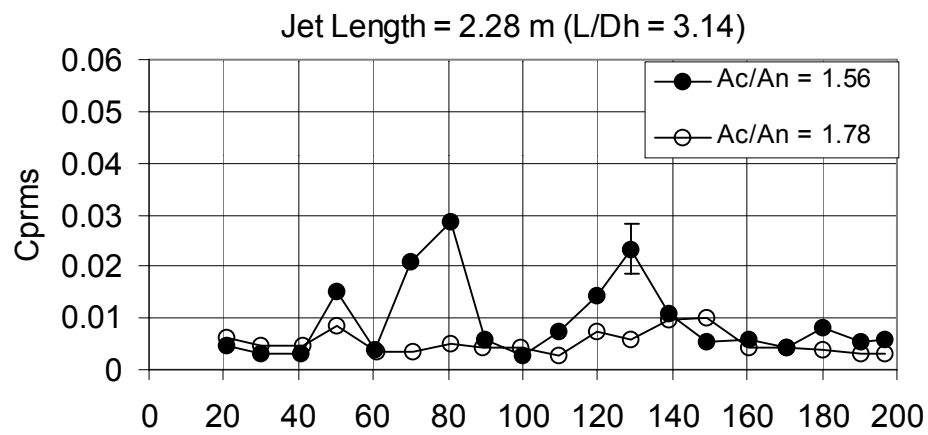
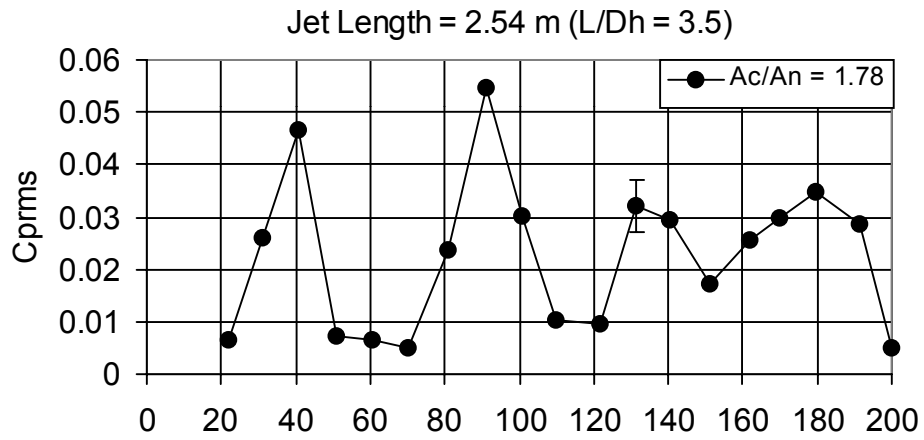


Figure 3: Pressure pulsation amplitudes.

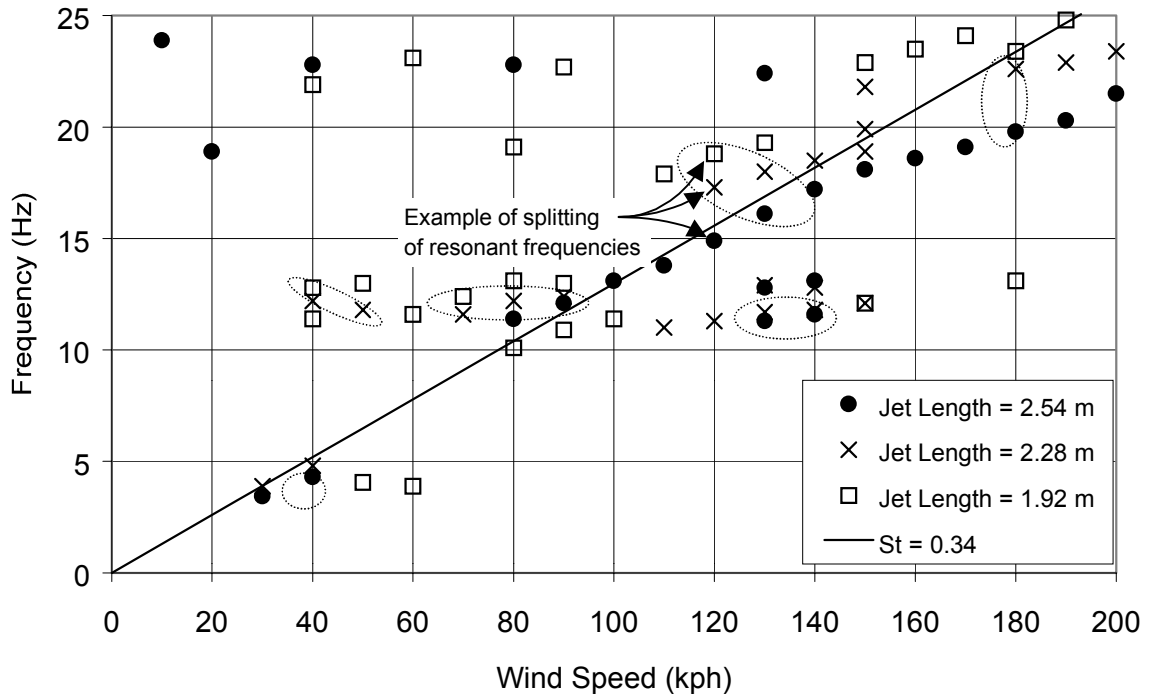


Figure 4: Pressure pulsation frequencies

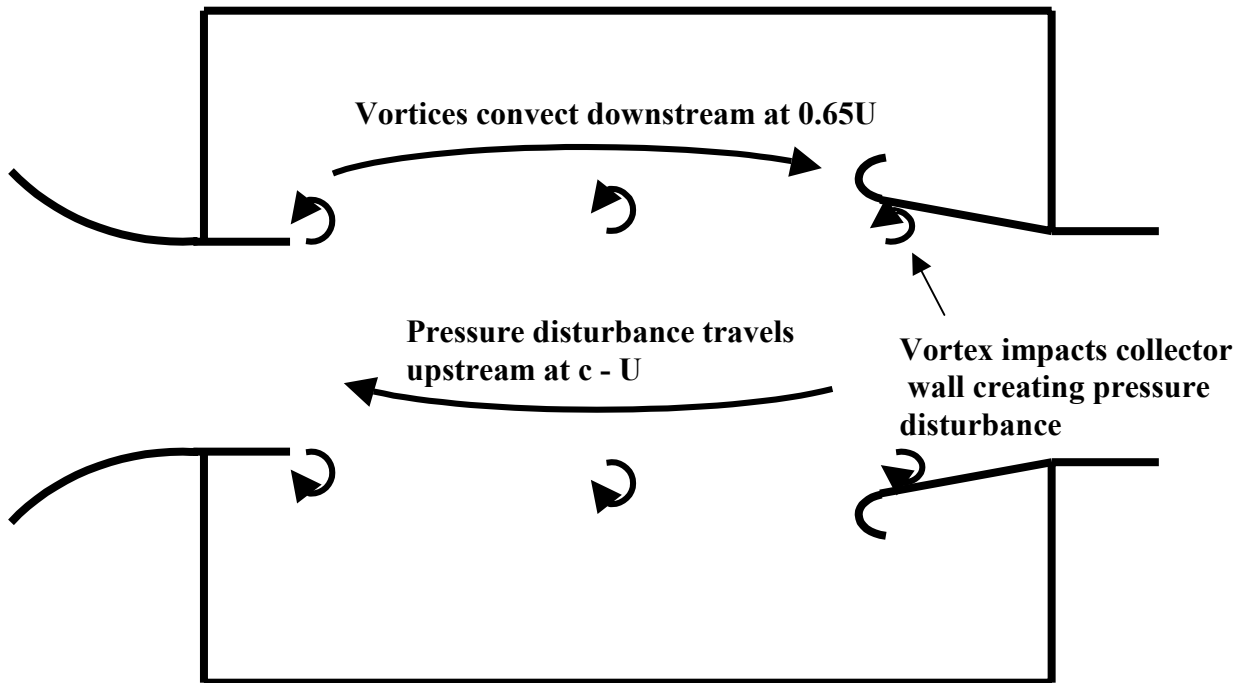


Figure 5: Drawing of edgetone feedback loop.

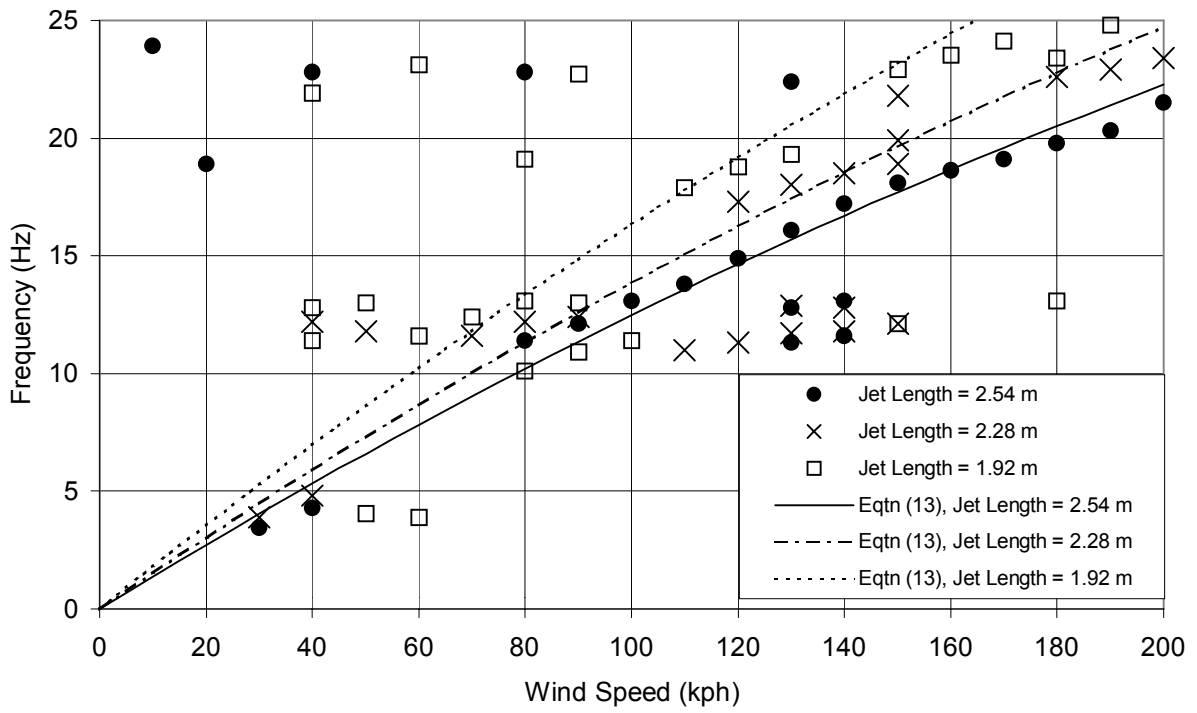


Figure 6: Comparison of predicted edgetone frequencies, Equation (13), with data.